Inorg. Chem. **2003**, *42*, 8385–8394

Synthesis, Structure, and Acid–Base and Redox Properties of a Family of New Ru(II) Isomeric Complexes Containing the Trpy and the Dinucleating Hbpp Ligands

Cristina Sens, Montserrat Rodríguez, Isabel Romero, and Antoni Llobet*

Departament de Química, Universitat de Girona, Campus de Montilivi, E-17071 Girona, Spain

Teodor Parella

Servei de RMN, Universitat Autònoma de Barcelona, Bellaterra, E-08193 Barcelona, Spain

Jordi Benet-Buchholz

Bayer Industry Services SUA-SPA X-ray Laboratory, Geb. Q18, Raum 490, Bayer AG, D-51368 Leverkusen, Germany

Received June 17, 2003

Three pairs of mononuclear geometrical isomers containing the ligand 3,5-bis(2-pyridyl)pyrazole (Hbpp) of general formula *in*- and *out*-$[Ru^{II}(Hbpp)(trpy)X]^{n+}$ (trpy = 2,2′:6′,2″-terpyridine; X = Cl, n = 1, **2a**,**b**; X = H_2O, n = 2, **3a**,**b**; X = py (pyridine), n = 2, **4a**,**b**) have been prepared through two different synthetic routes, isolated, and structurally characterized. The solid state structural characterization was performed by X-ray diffraction analysis of four complexes: **2a**–**4a** and **4b**. The structural characterization in solution was performed by means of 1D and 2D NMR spectroscopy for complexes **2a**,**b** and **4a**,**b** and coincides with the structures found in the solid state. All complexes were also spectroscopically characterized by UV–vis which also allowed us to carry out spectrophotometric acid–base titrations. Thus, a number of species were spectroscopically characterized with the same oxidation state but with a different degree of protonation. As an example, for **3a** three pK_a values were obtained: p$K_{a1}(Ru^{II})$ = 2.13, p$K_{a2}(Ru^{II})$ = 6.88, and p$K_{a3}(Ru^{II})$ = 11.09. The redox properties were also studied, giving in all cases a number of electron transfers coupled to proton transfers. The pH dependency of the redox potentials allowed us to calculate the pK_a of the complexes in the Ru(III) oxidation state. For complex **3a**, these were found to be p$K_{a1}(Ru^{III})$ = 0.01, p$K_{a2}(Ru^{III})$ = 2.78, and p$K_{a3}(Ru^{III})$ = 5.43. The oxidation state Ru(IV) was only reached from the Ru–OH_2 type of complexes **3a** or **3b**. It has also been shown that the Ru^{IV}═O species derived from **3a** is capable of electrocatalytically oxidizing benzyl alcohol with a second-order rate constant of k_{cat} = 17.1 M^{-1} s^{-1}.

Introduction

Polypyridyl complexes of Ru are being thoroughly investigated because of their multiple applications in fields of science including photophysics and photochemistry,[1] supramolecular chemistry,[2] catalysis,[3] and bioinorganic chemistry.[4] One important aspect of considerable interest is the design of complexes where their redox, absorption, and emission properties can be fine-tuned by simply changing the pH. In this respect, several proton switching induced phenomena have already been reported.[5] Another important aspect, especially from a catalytic perspective, is the design of Ru═O functional groups and analogues capable of reversibly accepting multiple electrons and protons within a relatively narrow potential range.[6] The capacity to modify their environment in order to induce electronic as well as steric effects will allow to fabricate tailored catalysts for specific reactions.

With all this in mind we have chosen to develop the Ru chemistry containing the 3,5-bis(2-pyridyl)pyrazole ligand

* To whom correspondence should be addressed. E-mail: antoni.llobet@udg.es.

10.1021/ic0346836 CCC: $25.00
Published on Web 11/15/2003

(Hbpp; see structural drawing),[7a] since it offers multiple protonation as well as coordination sites. Thus it can form mononuclear complexes as well as homo- and heterodinuclear complexes. In the case of the mononuclear complexes, they are nonsymmetric, and thus, different isomers with radically different orientations can be obtained which in turn can lead to completely differentiated reactivity patterns. These mononuclear complexes will also have a rich pH dependency due to the acid−base properties of the noncoordinated pyridyl group and of the pyrazolylic group, thus having protonation sites relatively remote from the metal center. In the case of the dinuclear complexes, the Hbpp acts as a bridging ligand, with the two metal centers strategically situated in close proximity and thus potentially leading to genuine cooperative effects.[8]

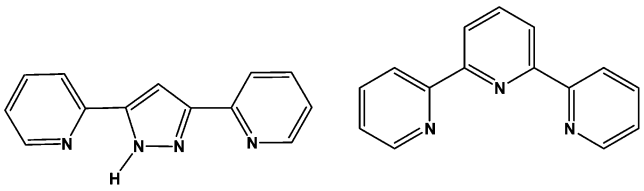

Hbpp **trpy**

In this paper, we present the synthesis, isolation, and structural characterization of the *in* and *out* geometrical isomers of general formula $[Ru^{II}(Hbpp)(trpy)X]^{n+}$ (trpy = 2,2′:6′,2″-terpyridine; X = Cl, $n = 1$ and X = H_2O or py (pyridine), $n = 2$). We have also studied their spectroscopic and electrochemical properties with a special attention to their pH dependency.

From here on the equatorial plane of these complexes is taken as the plane that ideally would contain the Hbpp ligand. The terms *in* and *out* are used to indicate whether another monodentate equatorial ligand (L = Cl, H_2O, or py) is oriented toward or away, respectively, from the center of the Hbpp ligand (see Scheme 1).

Experimental Section

Materials. All reagents used in the present work were obtained from Aldrich Chemical Co. and were used without further purification. Reagent grade organic solvents were obtained from SDS, and high purity deionized water was obtained by passing distilled water through a nanopure Mili-Q water purification system. $RuCl_3 \cdot 2H_2O$ was supplied by Johnson and Matthey Ltd. and was used as received.

Preparations. The starting complex, *cis(out),cis*-$[RuCl_2(Hbpp)(dmso)_2]$, **1**, and $[RuCl_3(trpy)]$ were prepared as described in the literature.[7] All synthetic manipulations were routinely performed under nitrogen atmosphere using Schlenk tubes and vacuum line techniques. Electrochemical experiments were performed under either N_2 or Ar atmosphere with degassed solvents.

3,5-Bis(2-pyridyl)pyrazole-1-carboxylic Acid tert-Butyl Ester, bpp-BOC. A 0.199 g (0.896 mmols) sample of Hbpp was dissolved in 30 mL of dichloromethane, and then, 0.137 mL (0.985 mmol) of triethylamine and 0.011 g (0.100 mmol) of 4-(dimethylamino)-pyridine were subsequently added to the solution under magnetic stirring. Afterward, 0.242 g (1.109 mmol) of di-*t*-butyl carbonate (di-BOC) was slowly added, and the resulting solution was magnetically stirred for 2 h at room temperature. Then, the volume of the solution was reduced to dryness in a rotary evaporator under low pressure. The residue was then dissolved in ethyl acetate and washed three times with a pH = 3 HCl aqueous solution. The organic phase was then dried over anhydrous $MgSO_4$ and reduced to dryness resulting in a white powder that was dried under vacuum. Yield 0.233 g (80.36%). Anal. Calcd for $C_{18}H_{18}N_4O_2$: C, 67.07; H, 5.63; N, 17.38. Found: C, 67.19; H, 5.85; N, 17.45. IR (cm^{-1}): ν, 1766 m, 1593 w, 1456 m, 1302 m, 1226 m, 1140 m, 992 w, 846 m, 783 m, 744 w. ^1H NMR (500 MHz, $CDCl_3$): $\delta = 8.71$ (d, H10), 8.65 (d, H5), 8.25 (d, H2), 7.79 (t, H11), 7.78 (t, H4), 7.50 (d, H13), 7.34 (dd, H12), 7.28 (t, H3), 7.21 (s, H7), 1.4 (s, tert-butyl). ^{13}C NMR ($CDCl_3$): $\delta = 149.5$ (C10), 149.2 (C5), 137.1 (C11), 137.1 (C4), 124.2 (C13), 123.9 (C3), 123.4 (C12), 121.2 (C2), 109.8 (C7), 27.5 (tert-butyl). NMR assignment uses the same numbering scheme as for X-ray in this and all complexes described in the present work (see Figure 1A for the numbering scheme of **2a**, whose synthesis is described in the following paragraph). Mp 120.7−121.2 °C.

(1) (a) Thompson, D. W.; Schoonover, J. R.; Graff, D. K.; Fleming, C. N.; Meyer, T. J. *J. Photochem. Photobiol., A* **2000**, *137*, 131. (b) Toma, H. E.; Serrasqueiro, R. M.; Rocha, R. C.; Demets, G. J. F.; Winnischofer, H.; Araki, K.; Ribeiro, P. E. A.; Donnici, C. L. *J. Photochem. Photobiol., A* **2000**, *135*, 185. (c) Keefe, M. H.; Benkstein, K. D.; Hupp, J. T. *Coord. Chem. Rev.* **2000**, *205*, 201. (d) Tyson, D. S.; Luman, C. R.; Zhou, X.; Castellano, F. N. *Inorg. Chem.* **2001**, *40*, 4063. (e) Balzani, V.; Juris, A. *Coord. Chem. Rev.* **2001**, *211*, 97. (f) Dattelbaum D. M.; Hartshorn, C. M.; Meyer, T. J. *J. Am. Chem. Soc.* **2002**, *124*, 4938. (g) Fleming, C. N.; Dupray, L. M.; Papanikolas, J. M.; Meyer, T. J. *J. Phys. Chem. A* **2002**, *106*, 2328. (h) Ballardini, R.; Balzani, V.; Credi, A.; Gandolfi, M. T.; Venturi, M. *Int. J. Photoenergy* **2001**, *3*, 63. (i) Baranoff, E.; Collin, J.-P.; Furusho, J.; Furusho, Y.; Laemmel, A.-C.; Sauvage, J.-P. *Inorg. Chem.* **2002**, *41*, 1215.

(2) Ashton, P. R.; Ballardini, R.; Balzani, V.; Credi, A.; Dress, K. R.; Ishow, E.; Kleverlaan, C. J.; Kocian, O.; Preece, J. A.; Spencer, N.; Stoddart, J. F.; Venturi, M.; Wenger, S. *Chem. Eur. J.* **2000**, *6*, 3558.

(3) (a) Murahashi, S.-I.; Takaya, H.; Naota, T. *Pure Appl. Chem.* **2002**, *74*, 19. (b) Naota, T.; Takaya, H.; Murahashi, S.-I. *Chem. Rev.* **1998**, *98*, 2599. (c) Rodríguez, M.; Romero, I.; Llobet, A.; Deronzier, A.; Biner, M.; Parella, T.; Soteckli-Evans, H. *Inorg. Chem.* **2001**, *40*, 4150. (d) Jauregui-Haza, U. J.; Dessoudeix, M.; Kalck, P.; Wilhelm, A. M.; Delmas, H. *Catal. Today* **2001**, *66*, 297.

(4) (a) Kelly, S. O.; Barton, J. K. *Science* **1999**, *238*, 375. (b) Hall, D. B.; Holmlin, R. E.; Barton, J. K. *Nature* **1996**, *384*, 731. (c) Burrows, C. J.; Muller, J. G. *Chem. Rev.* **1998**, *98*, 1109. (d) Schuster, G. B. *Acc. Chem. Res.* **2000**, *33*, 253. (e) Weatherly, S. C.; Yang, I. V.; Thorp, H. H. *J. Am. Chem. Soc.* **2001**, *123*, 1236.

(5) (a) Haga, M.; Ali, M. M.; Maegawa, H.; Nozaki, K.; Yoshimura, A.; Ohno, T. *Coord. Chem. Rev.* **1994**, *94*, 99. (b) Haga, M.; Ali, M. M.; Arakawa, R. *Angew. Chem., Int. Ed. Engl.* **1996**, *35*, 76. (c) Baitalik, S.; Florke, U.; Nag, K. *Inorg. Chem.* **1999**, *38*, 3296. (d) Lodeiro, C.; Pina, F.; Parola, A. J.; Bencini, A.; Bianchi, A.; Bazzicalupi, C.; Ciattini, S.; Giorgi, C.; Masotti, A.; Valtancoli, B.; Demelo, J. S. *Inorg. Chem.* **2001**, *40*, 6813.

(6) (a) Stultz, L. K.; Huynh, M. H. V.; Binstead, R. A.; Curry, M.; Meyer, T. J. *J. Am. Chem. Soc.* **2000**, *122*, 5984. (b) Lebeau, E. L.; Meyer, T. J. *Inorg. Chem.* **1999**, *38*, 2174. (c) Che, C. M.; Lai, T. F.; Wong, K. Y. *Inorg. Chem.* **1987**, *26*, 2289. (d) Muller, J. H.; Acquaye, J. H.; Takeuchi, K. J. *Inorg. Chem.* **1992**, *31*, 4552. (e) Gerli, A.; Reedijk, J.; Lakin, M. T.; Spek, A. L. *Inorg. Chem.* **1995**, *34*, 1836. (f) Hua, X.; Shang, M.; Lappin, A. G. *Inorg. Chem.* **1997**, *36*, 3735. (g) Llobet, A.; Doppelt, P.; Meyer, T. J. *Inorg. Chem.* **1998**, *27*, 514. (h) Rodriguez, M.; Romero, I.; Llobet, A.; Deronzier, A.; Biner, M.; Parella, T.; Stoeckli-Evans, H. *Inorg. Chem.* **2001**, *40*, 4150. (i) Shiotsuki, M.; Miyai, H.; Ura, Y.; Suzuki, T.; Kondo, T.; Mitsudo, T. *Organometallic* **2002**, *21*, 4960−4964. (j) Huynh, M. H. V.; Witham, L. M.; Lasker, J. M.; Wetzler, M.; Mort, B.; Jameson, D. L.; White P. S.; Takeuchi, K. J. *J. Am. Chem. Soc.* **2003**, *125*, 308−309.

(7) (a) Sens, C.; Rodríguez, M.; Romero, I.; Llobet, A.; Parella, T.; Sullivan, B. P.; Benet-Buchholz, J. *Inorg. Chem.* **2003**, *42*, 2040. (b) Sullivan, B. P.; Calvert, J. M.; Meyer, T. J. *Inorg. Chem.* **1980**, *19*, 1404.

(8) (a) Catalano, V. J.; Craig, T. J.; *Inorg. Chem.* **2003**, *42*, 321. (b) Catalano, V. J.; Heck, R. A.; Immoos, C. E.; Ohman, A.; Hill, M. *Inorg. Chem.* **1998**, *37*, 2150.

Scheme 1. Synthetic Pathways

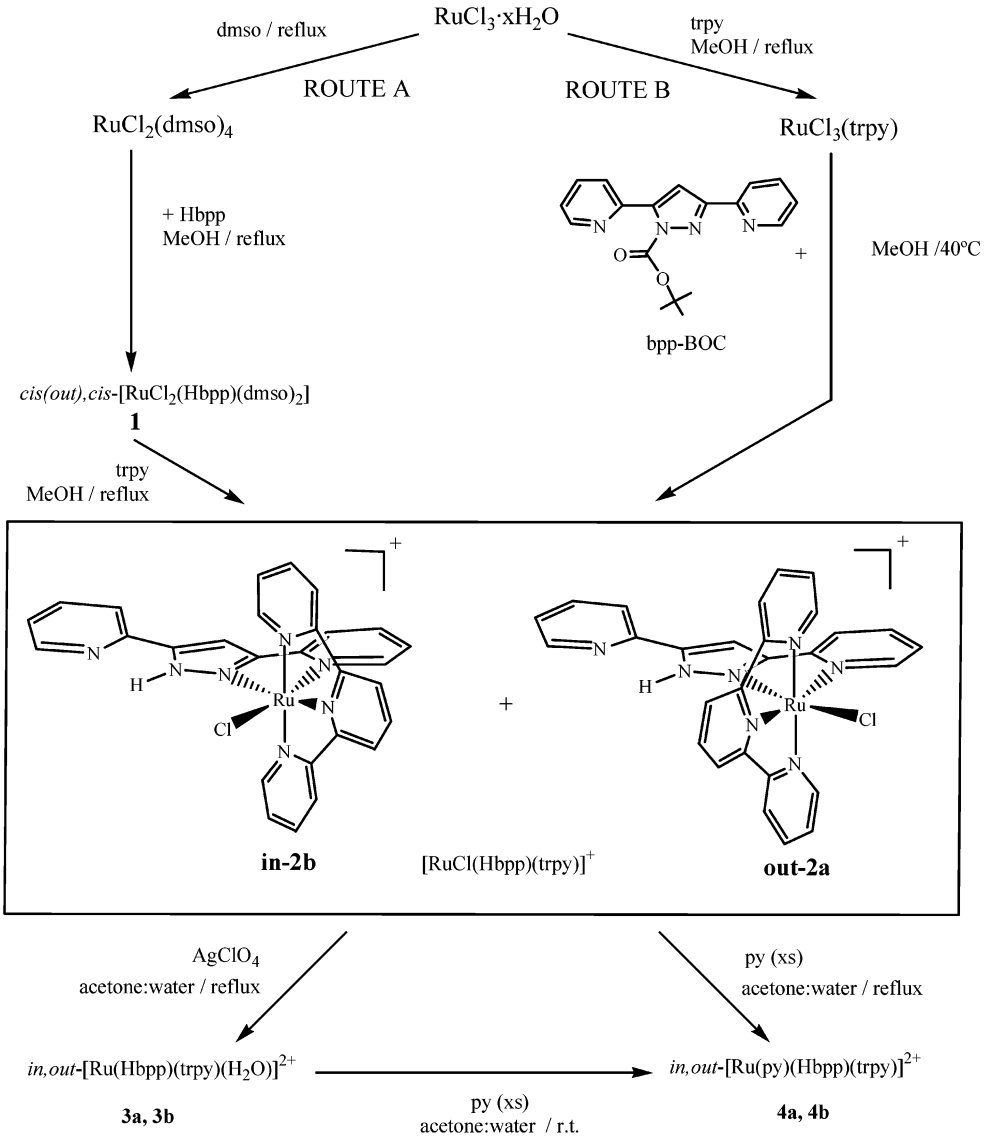

***out*-[Ru^{II}(Cl)(H$_2$bpp)(trpy)](PF$_6$)(Cl)·H$_2$O, 2a·H$_2$O, and *in*-[Ru^{II}(Cl)(H$_2$bpp)(trpy)](PF$_6$)(Cl)·H$_2$O, 2b·H$_2$O. Route A.** A 300 mg (0.545 mmol) sample of **1** and a 128 mg (0.548 mmol) sample of trpy were placed in a 250 mL round-bottom flask together with 150 mL of MeOH, and the mixture was refluxed overnight. The resulting solution was concentrated on a rotary evaporator until a yellow solid, corresponding to residual complex **1**, precipitated out of the solution. The mixture was then cooled on an ice bath for 30 min and filtered through a frit. The solution was then evaporated to dryness, and the resulting solid was purified over neutral alumina using a mixture CH_2Cl_2/CH_3CN (1:1, v/v) as eluent. The first pink fraction, corresponding to *out*-[Ru^{II}Cl(bpp)(trpy)], was evaporated to dryness, and the resulting solid was dissolved in the minimum amount of MeOH. Some drops of a 0.5 M HCl solution were added to ensure the complete protonation of the bpp ligand, followed by 1 mL of a saturated aqueous NH_4PF_6 solution. The volume was then reduced on a rotary evaporator until a precipitate appeared. The mixture was cooled on an ice bath for 30 min, and the solid was filtered on a frit, washed with cold water (3 × 10 mL) and diethyl ether (3 × 10 mL), and dried in a vacuum. Yield: 181 mg of a dark brown complex **2a** (42.0%). Anal. Calcd for $C_{28}H_{22}Cl_2F_6N_7PRu·H_2O$: C, 42.49; H, 3.06; N, 12.39. Found: C, 42.80; H, 3.28; N, 12.41. IR (KBr pellet, cm^{-1}): ν, 1598 m, 1448 m, 1387 w, 845 s, 772 m, 558 m. ^{1}H NMR (500 MHz, MeOD): δ = 10.07 (d, $^3J_{5-4}$ = 5.15 Hz, H5), 8.60 (d, $^3J_{23-22}$ = $^3J_{21-22}$ = 7.7 Hz, H23, H21), 8.50 (d, $^3J_{15-16}$ = $^3J_{25-26}$ = 8.1 Hz, H15, H25), 8.47 (d, $^3J_{2-3}$ = 7.5 Hz, H2), 8.44 (d, $^3J_{10-11}$ = 4.5 Hz, H10), 8.29 (t, $^3J_{3-2}$ = 7.5 Hz, $^3J_{3-4}$ = 7.65 Hz, H3), 8.13 (t, $^3J_{22-23}$ = $^3J_{22-21}$ = 7.7 Hz, H22), 7.93 (t, $^3J_{16-15}$ = $^3J_{26-25}$ = 8.1 Hz, $^3J_{16-17}$ = $^3J_{26-27}$ = 6.45 Hz, H16, H26), 7.86 (t, $^3J_{4-5}$ = 5.15 Hz, $^3J_{4-3}$ = 7.65 Hz, H4), 7.82 (t, $^3J_{12-13}$ = 8.8 Hz, $^3J_{12-11}$ = 6.6 Hz, H12), 7.74 (d, $^3J_{18-17}$ = $^3J_{28-27}$ = 4.9 Hz, H18, H28), 7.69 (d, $^3J_{13-12}$ = 8.8 Hz, H13), 7.67 (s, H7), 7.35 (t, $^3J_{17-16}$ = $^3J_{27-26}$ = 6.45 Hz, $^3J_{17-18}$ = $^3J_{27-28}$ = 4.9 Hz, H17, H27), 7.29 (t, $^3J_{11-12}$ = 6.6 Hz, $^3J_{11-10}$ = 4.5 Hz, H11). NOESY (500 MHz, MeOD): δ = 7.67−7.69 (H7−H13), 7.67−8.47 (H7−H2), 7.74−10.07 (H18−H5, H28−H5), 8.60−8.50 (H23−H15, H21−H25). ESI-MS (CH_3CN): m/z = 592.2 ([M − PF_6]$^+$).

The fractions remaining on the column, which correspond to the *in* isomer together with [Ru(trpy)$_2$]$^{2+}$ and other secondary products, were eluted with methanol and purified over a silica column using MeOH, with some drops of NH_4OH, as eluent. The first eluted fraction from this second column corresponds to [Ru(trpy)$_2$]$^{2+}$, and the second one is the deprotonated **2b** complex. The solution

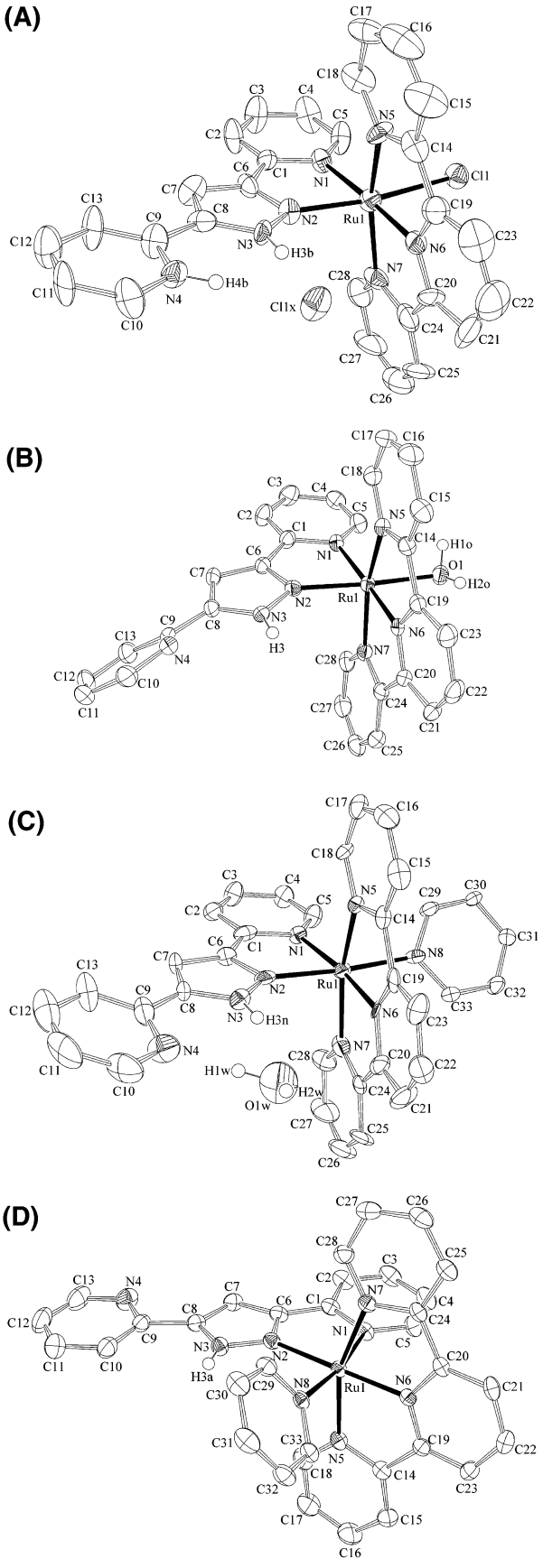

Figure 1. X-ray structures (ORTEP plots with ellipsoids at 50% probability level) and labeling scheme for (A) **2a·4.63H$_2$O**, (B) **3a·3H$_2$O**, (C) **4a·H$_2$O**, and (D) **4b·MeCN**.

containing **2b** was evaporated to dryness and afterward dissolved in MeOH containing a few drops of 0.5 M HCl and 1 mL of a saturated NH_4PF_6 aqueous solution. The volume was then again reduced on a rotary evaporator until a solid precipitated out of the solution. The mixture was then cooled on an ice bath for 30 min and the solid filtered on a frit, washed with cold water (3 × 10 mL) and ether (3 × 10 mL), and dried in a vacuum. Yield: 46 mg of brown-orange complex **2b** (10.7%). Anal. Calcd for $C_{28}H_{22}Cl_2F_6N_7PRu\cdot H_2O$: C, 42.49; H, 3.06; N, 12.39. Found: C, 42.27; H, 3.05; N, 12.31. IR (KBr pellets, cm^{-1}): ν, 1636 m, 1448 m, 1387 w, 844 s, 768 m, 558 m. ^{1}H NMR (500 MHz, acetonitrile-d_3): δ 8.83 (dd, $^3J_{10-11} = 4.55$ Hz, $^4J_{10-12} = 1.05$ Hz, H10); 8.63 (td, $^3J_{12-11} = 9.1$ Hz, $^3J_{12-13} = 6.0$ Hz, $^4J_{12-10} = 1.05$ Hz, H12), 8.58 (d, $^3J_{23-22} = {}^3J_{21-22} = 8.05$ Hz, H23, H21), 8.51 (d, $^3J_{13-12} = 6.0$ Hz, H13), 8.46 (dd, $^3J_{15-16} = {}^3J_{25-26} = 8.05$ Hz, $^4J_{15-17} = {}^4J_{25-27} = 1.25$ Hz, H15, H25), 8.35 (t, $^3J_{22-23} = {}^3J_{22-21} = 8.05$ Hz, H22), 8.24 (s, H7), 8.13 (dd, $^3J_{4-3} = 7.85$ Hz, $^4J_{4-2} = 1.4$ Hz, H4), 8.05 (td, $^3J_{16-15} = {}^3J_{26-25} = 8.05$, $^3J_{16-17} = {}^3J_{26-27} = 7.8$ Hz, $^4J_{16-18} = {}^4J_{26-28} = 1.4$ Hz, H16, H26), 7.99 (t, $^3J_{11-10} = 4.55$ Hz, $^3J_{11-12} = 9.1$ Hz, H11), 7.92 (dd, $^3J_{18-17} = {}^3J_{28-27} = 5.4$ Hz, $^4J_{18-16} = {}^4J_{28-26} = 1.4$ Hz, H18, H28), 7.84 (td, $^3J_{3-2} = 7.85$ Hz, $^3J_{3-4} = 7.9$ Hz, $^4J_{3-5} = 1.2$ Hz, H3), 7.42 (ddd, $^3J_{17-16} = {}^3J_{27-26} = 7.8$ Hz, $^3J_{17-18} = {}^3J_{27-28} = 5.4$ Hz, $^4J_{17-15} = {}^4J_{27-25} = 1.25$ Hz, H17, H27), 7.23 (dd, $^3J_{5-4} = 5.25$ Hz, $^4J_{5-3} = 1.2$ Hz, H5), 7.05 (ddd, $^3J_{4-3} = 7.9$ Hz, $^3J_{4-5} = 5.25$ Hz, $^4J_{4-2} = 1.4$ Hz, H4). NOESY (500 MHz, acetonitrile-d_3): $\delta = 8.24-8.51$ (H7−H13), 8.24−8.13 (H7−H2), 8.58−8.46 (H23−H15, H21−H25). ESI-MS (CH_3CN): $m/z = 591.9$ ($[M - PF_6]^+$).

Route B. A 0.317 g (0.720 mmol) sample of $[RuCl_3(trpy)]$ was placed in a flask containing 25 mL of MeOH. Then, a 61.1 mg sample of LiCl was added together with 0.2 mL (1.438 mmol) of NEt_3. The resulting mixture was magnetically stirred at room temperature under nitrogen atmosphere for 30 min. Then, a 0.233 g (0.720 mmol) sample of bpp-BOC was added and the reaction mixture gently heated at 40 °C overnight. The resulting solution is then filtered hot and the volume reduced to dryness at low pressure. The separation and purification procedures are now exactly the same as those described for route A. Yields: 0.257 mg of **2a** (60.45%) and 0.107 g of **2b** (20.13%).

***out*-[Ru^{II}(Hbpp)(trpy)(OH$_2$)](ClO$_4$)$_2$, 3a·H$_2$O.** A 50.7 mg (0.064 mmol) sample of **2a** and a 13.3 mg (0.064 mmol) sample of $AgClO_4$ were placed in a 25 mL round-bottom flask together with 10 mL of a 1:3 water/acetone solution (v/v). The resulting solution was refluxed for 1.5 h and then cooled on an ice bath. AgCl precipitated out of the solution and was filtered over Celite. Afterward, a few drops of a saturated aqueous $NaClO_4$ solution was added and the volume reduced on a rotary evaporator, with the temperature kept below 30 °C, until the formation of a precipitate. The mixture was then cooled on an ice bath for 30 min and the solid obtained filtered through a frit, washed with cold water (3 × 10 mL) and ether (3 × 10 mL), and dried in a vacuum. A dark brown solid was obtained. Yield: 45 mg of complex **3a** (88.8%). Anal. Calcd for $C_{28}H_{23}Cl_2N_7O_9Ru\cdot H_2O$: C, 42.49; H, 3.18; N, 12.39. Found: C, 42.19; H, 2.95 N, 12.10. IR (KBr pellet, cm^{-1}): ν, 1626 w, 1599 m, 1448 m, 1043 s, 1111 s, 108 v8 f, 772 m, 627 m. ESI-MS (MeOH): $m/z = 674.2$ ($[M - ClO_4]^+$), 656.1 ($[M - H_2O - ClO_4]^+$), 574.1 ($[M - H^+ - 2ClO_4]^+$).

***in*-[Ru^{II}(Hbpp)(trpy)(OH$_2$)](ClO$_4$)$_2$, 3b·H$_2$O.** This complex was prepared following the same procedure described for **3a** but using compound **2b** instead of **2a** as the starting material. A dark brown solid was obtained. Yield: 40 mg of **2b** (78.1%). Anal. Calcd for $C_{28}H_{23}Cl_2N_7O_9Ru\cdot H_2O$: C, 42.49; H, 3.18; N, 12.39. Found: C, 42.47; H, 2.94; N, 12.08. IR (KBr pellet, cm^{-1}): ν, 1595 m, 1446

m, 1384 w, 1243 w, 1143 s, 1113 s, 1087 s, 769 m, 627 m. ESI-MS (MeOH): m/z = 677.9 ($[M - H^+ - H_2O + Na^+ - ClO_4]^+$), 655.8 ($[M - H_2O - ClO_4]^+$).

***out*-[Ru^{II}(py)(Hbpp)(trpy)](PF$_6$)$_2$·H$_2$O, 4a·H$_2$O.** A 53.7 mg (0.068 mmol) sample of **2a** and 0.15 mL (1.85 mmol) of pyridine were placed in a 25 mL round-bottom flask together with 10 mL of a 1:3 water/acetone solution (v/v). The resulting solution was refluxed for 4 h and filtered hot on a Büchner funnel. Then, 0.5 mL of a saturated NH_4PF_6 aqueous solution was added to the filtrate, and the volume was reduced on a rotary evaporator until a solid precipitated out of the solution. The microcrystalline red solid was filtered through a frit, washed with cold water (3 × 10 mL) and ether (3 × 10 mL), and dried in a vacuum. Yield: 48 mg of **4a** (75.0%). Anal. Calcd for $C_{33}H_{26}F_{12}N_8P_2Ru·H_2O$: C, 42.00; H, 2.99; N, 11.87. Found: C, 41.73; H, 2.88; N, 12.08. IR (KBr pellet, cm^{-1}): ν, 1601 m, 1448 m, 840 f, 765 m, 558 m. ^{1}H NMR (500 MHz, acetonitrile-d_3): δ 8.49 (d, $^3J_{23-22} = {}^3J_{21-22}$ = 8.2 Hz, H23, H21), 8.48 (dd, $^3J_{5-4}$ = 3.3 Hz, $^4J_{5-3}$ = 1.4 Hz, H5), 8.44 (dd, $^3J_{2-3}$ = 7.7 Hz, $^4J_{2-4}$ = 1.4 Hz, H2), 8.44 (dd, $^3J_{15-16} = {}^3J_{25-26}$ = 7.7 Hz, $^4J_{15-17} = {}^4J_{25-27}$ = 1.4 Hz, H15, H25), 8.40 (dd, $^3J_{10-11}$ = 4.2 Hz, $^4J_{10-12}$ = 1.4 Hz, H10), 8.31 (td, $^3J_{3-4}$ = 7.9 Hz, $^3J_{3-2}$ = 7.7 Hz, $^4J_{3-5}$ = 1.4 Hz, H3), 8.16 (t, $^3J_{22-23} = {}^3J_{22-21}$ = 8.2 Hz, H22), 8.04 (td, $^3J_{16-15} = {}^3J_{26-25}$ = 7.7 Hz, $^3J_{16-17} = {}^3J_{26-27}$ = 8.05 Hz, $^4J_{16-18} = {}^4J_{26-28}$ = 1.4 Hz, H16, H26), 7.85 (td, $^3J_{12-11}$ = 8.3 Hz, $^3J_{12-13}$ = 7.45 Hz, $^4J_{12-10}$ = 1.4 Hz, H12), 7.83 (dd, $^3J_{18-17} = {}^3J_{28-27}$ = 4.2 Hz, $^4J_{18-16} = {}^4J_{28-26}$ = 1.4 Hz, H18, H28), 7.79 (dt, $^3J_{31-30} = {}^3J_{31-32}$ = 7.7 Hz, $^4J_{31-29} = {}^4J_{31-33}$ = 1.4 Hz, H31), 7.71 (ddd, $^3J_{4-5}$ = 3.3 Hz, $^3J_{4-3}$ = 7.9 Hz, $^4J_{4-2}$ = 1.4 Hz, H4), 7.66 (dd, $^3J_{13-12}$ = 7.45 Hz, $^4J_{13-11}$ = 1.05 Hz, H13), 7.65 (dd, $^3J_{29-30} = {}^3J_{33-32}$ = 6.45 Hz, $^4J_{29-31} = {}^4J_{33-31}$ = 1.4 Hz, H29, H33), 7.64 (s, H7), 7.45 (ddd, $^3J_{17-16} = {}^3J_{27-26}$ = 8.05, $^3J_{17-18} = {}^3J_{27-28}$ = 4.2 Hz, $^4J_{17-15} = {}^4J_{27-25}$ = 1.4 Hz, H17, H27), 7.32 (ddd, $^3J_{11-10}$ = 4.2 Hz, $^3J_{11-12}$ = 8.3 Hz, $^4J_{11-13}$ = 1.05 Hz, H11), 7.21 (dd, $^3J_{30-29} = {}^3J_{32-33}$ = 6.45, $^3J_{30-31} = {}^3J_{32-31}$ = 7.7 Hz, H30, H32). NOESY (500 MHz, acetonitrile-d_3): δ = 7.64−7.66 (H7−H13), 7.64−8.44 (H7−H2), 7.83−8.48 (H18−H5, H28−H5), 8.49−8.44 (H23−H15, H21−H25). ESI-MS (CH_3CN): m/z = 781.2 ($[M - PF_6]^+$), 635.3 ($[M - H^+ - 2PF_6]^+$).

***in*-[Ru^{II}(py)(Hbpp)(trpy)](PF$_6$)$_2$·H$_2$O, 4b·H$_2$O.** This complex was synthesized following the same procedure described for **4a** but with compound **2b** instead of **2a**. A brown solid was obtained. Yield: 35 mg of **4b** (55.5%). Anal. Calcd for $C_{33}H_{26}F_{12}N_8P_2Ru·H_2O$: C, 42.00; H, 2.99; N, 11.87. Found: C, 41.83; H, 3.01; N, 12.09. IR (KBr pellet, cm^{-1}): ν, 1602 m, 1448 m, 845 s, 769 m, 558 m. ^{1}H NMR (500 MHz, acetonitrile-d_3): δ 8.70 (d, $^3J_{13-12}$ = 4.7 Hz, H13), 8.56 (d, $^3J_{21-22} = {}^3J_{23-22}$ = 8.25 Hz, H21, H23), 8.44 (d, $^3J_{25-26} = {}^3J_{15-16}$ = 7.9 Hz, H25, H15), 8.23 (t, $^3J_{22-21} = {}^3J_{22-23}$ = 8.25 Hz, H22), 8.11 (d, $^3J_{2-3}$ = 7.85 Hz, H2), 8.07 (s, H7), 8.05 (d, $^3J_{10-11}$ = 7 Hz, H10), 8.05 (t, $^3J_{11-10}$ = 7 Hz, H11), 8.02 (d, $^3J_{28-27} = {}^3J_{18-17}$ = 5.25 Hz, H28, H18), 8.01 (t, $^3J_{26-25} = {}^3J_{16-15}$ = 7.9 Hz, $^3J_{26-27} = {}^3J_{16-17}$ = 7.55 Hz, H26, H16), 7.94 (d, $^3J_{29-30} = {}^3J_{33-32}$ = 5.05 Hz, H29, H33), 7.79 (t, $^3J_{3-2}$ = 7.85 Hz, $^3J_{3-4}$ = 6.6 Hz, H3), 7.77 (t, $^3J_{31-30} = {}^3J_{31-32}$ = 8.9 Hz, H31), 7.50 (dd, $^3J_{12-13}$ = 4.7 Hz, $^3J_{12-11}$ = 7 Hz, H12), 7.42 (t, $^3J_{27-28} = {}^3J_{17-18}$ = 5.25 Hz, $^3J_{27-26} = {}^3J_{17-16}$ = 7.55 Hz, H27, H17), 7.21 (t, $^3J_{30-29} = {}^3J_{32-33}$ = 5.05 Hz, $^3J_{30-31} = {}^3J_{32-31}$ = 8.9 Hz, H30, H32), 7.14 (d, $^3J_{5-4}$ = 5.8 Hz, H5), 6.97 (t, $^3J_{4-3}$ = 6.6 Hz,.$^3J_{4-5}$ = 5.8 Hz, H4). NOESY (500 MHz, acetonitrile-d_3): δ = 8.55−8.43 (H21−H25, H23−H15). ESI-MS (CH_3CN): m/z = 781.8 ($[M - PF_6]^+$), 635.0 ($[M - H^+ - 2PF_6]^+$).

Instrumentation and Measurements. IR spectra were recorded on an Mattson Satellite FT-IR with KBr pellets or using a MKII Golden Gate single reflection ATR system. UV−vis spectroscopy was performed in a Cary 50 Scan (Varian) UV−vis spectrophotometer with 1 cm quartz cells. pH measurements were done using a Micro-pH-2000 from Crison. Cyclic voltammetric (CV) experiments were performed in a PAR 263A EG&G potentiostat or in an IJ-Cambria IH-660 potentiostat using a three electrode cell. Glassy carbon disk electrodes (3 mm diameter) from BAS were used as working electrode, platinum wire was used as auxiliary, and SSCE was used as the reference electrode (all the potentials given in this work are always with regard to this reference electrode). Unless explicitly mentioned, all cyclic voltammograms presented in this work were recorded at 100 mV/s scan rate under nitrogen atmosphere, and complex concentration was approximately 1 mM. The complexes were dissolved in previously degassed solvents containing the necessary amount of supporting electrolyte to yield a 0.1 M ionic strength solution. In acetonitrile, (n-Bu_4N)(PF_6), TBAH, was used as supporting electrolyte. In aqueous solutions, the pH was adjusted from 0 to 2 with HCl. Potassium chloride was added to keep a minimum ionic strength of 0.1 M. From pH 2−10, 0.1 M phosphate buffers were used, and from pH 10−12 diluted, CO_2 free, NaOH. All $E_{1/2}$ values reported in this work were estimated from cyclic voltammetry as the average of the oxidative and reductive peak potentials ($E_{p,a} + E_{p,c}$)/2. Bulk electrolyses were carried out in a three-compartment cell using carbon felt from SOFACEL as the working electrode.

The ^{1}H NMR spectroscopy was performed on a Bruker 500 MHz. Samples were run in MeOH-d_4 or acetonitrile-d_3, with internal references (residual protons and/or tetramethylsilane). Elemental analyses were performed using a CHNS-O elemental analyzer EA-1108 from Fisons. The ESI-MS experiments were performed on a Navigator LC/MS chromatograph from Thermo Quest Finigan, using methanol or acetonitrile as a mobile phase.

For acid−base spectrophotometric titration, (3−4) × 10^{-5} M buffered aqueous solutions of the complexes were used. The pH of the different solutions was adjusted by adding small volumes (approximately 10 μL) of 4 M NaOH in order to produce a negligible overall volume change. Redox spectrophotometric titrations were performed by sequential addition of a $(NH_4)_2[Ce^{IV}(NO_3)_6]$ 0.1 M solution in $HClO_4$ to the complex.

X-ray Structure Determinations. Crystals of *out*-[Ru^{II}(Cl)-(H_2bpp)(trpy)](PF_6)(Cl), **2a**, were grown from different solvents as small red or brown plates at room temperature. These crystals are highly sensitive to losing solvent immediately after removing from their mother liquor. After different trials, a data set of moderate quality could be acquired from a small crystal (150 × 100 × 15 μm^3) obtained from dichloromethane. The measured crystal was prepared under inert conditions immersed in perfluoropolyether as protecting oil for manipulation. Black crystals of *out*-[Ru^{II}(Hbpp)-(trpy)(OH_2)](ClO_4)$_2$, **3a**, could be grown by slow evaporation of water at room temperature. Crystals of *out*-[Ru^{II}(py)(Hbpp)(trpy)]-(PF_6)$_2$, **4a**, and *in*-[Ru^{II}(py)(Hbpp)(trpy)](PF_6)$_2$, **4b**, could be obtained as small red needles (350 × 20 × 10 μm^3 in the case of **4a**) by slow diffusion of diethyl ether into an acetonitrile solution of the complex.

Data Collection. Measurements of **2a**, **3a**, **4a**, and **4b** were made on a Siemens P4 diffractometer equipped with a SMART-CCD-1000 area detector, a MACScience Co. rotating anode with Mo Kα radiation, a graphite monochromator, and a Siemens LT2 low temperature device (T = −120 °C). Full-sphere data collection was used with ω and φ scans. Programs used: data collection, Smart V. 5.060 (BrukerAXS 1999); data reduction, Saint+ Version 6.02 (Bruker AXS 1999); absorption correction, SADABS (Bruker AXS 1999).

Table 1. Crystal Data for Complexes **2a**−**4a** and **4b**

	2a·4.63H_2O	**3a**·3H_2O	**4a**·H_2O	**4b**·MeCN
empirical formula	$C_{28}H_{22}Cl_2F_6N_7O_{4.63}PRu$	$C_{28}H_{29}Cl_2N_7O_{12}Ru$	$C_{33}H_{28}F_{12}N_8OP_2Ru$	$C_{35}H_{29}F_{12}N_9P_2Ru$
fw	847.47	827.55	943.64	966.68
cryst syst	triclinic	monoclinic	monoclinic	monoclinic
space group	*P*1	*C*2/c	$P2_1/c$	$P2_1/c$
a, Å	8.7598(13)	24.596(5)	21.252(3)	15.7019(5)
b, Å	14.059(2)	11.394(2)	8.5801(12)	16.8008(6)
c, Å	20.349(3)	25.071(5)	21.142(3)	14.2793(5)
α, deg	91.277(6)	90	90	90
β, deg	92.076(8)	111.006(7)	114.132(4)	92.2030(10)
γ, deg	101.509(6)	90	90	90
V, Å^3	2453.0(6)	6559(2)	3518.2(2)	3764.2(2)
formula units/cell	2	8	4	4
T, K	153(2)	153(2)	153(2)	153(2)
λ(Mo Kα), Å	0.71073	0.71073	0.71073	0.71073
ρ_{calcd}, g cm^{-3}	1.147	1.676	1.782	1.706
μ, mm^{-1}	0.517	0.715	0.644	0.603
R1[a]	0.0828	0.0400	0.0554	0.0516
wR2[b]	0.2087	0.0745	0.0855	0.0948

[a] $R1 = \sum||F_o| - |F_c||/\sum|F_o|$. [b] $wR2 = [\sum\{w(F_o^2 - F_c^2)^2\}/\sum\{w(F_o^2)^2\}]^{1/2}$, on $w = 1/[\sigma^2F_o^2 + (0.0377P)^2 + 1.65P]$; $P = (F_o^2 + 2F_c^2)/3$.

Structure Solution and Refinement. SHELXTL Version 5.10 (Sheldrick, 1998) was used. All discussed hydrogen distances are noncorrected.[9]

Results and Discussion

Synthesis and Solid State Structure. The new Ru−Cl complexes **2a** and **2b** reported in this work have been prepared following two different synthetic routes that are outlined in Scheme 1. These two routes differ mainly in the order of the sequential addition of the Hbpp and trpy ligands to the initial ruthenium complex. In this way, we use the *cis(out)cis*-[$RuCl_2$(Hbpp)$(dmso)_2$], **1**, and [$RuCl_3$(trpy)] complexes, previously described by ourselves[7a] and Meyer et al.,[7b] respectively, as synthetic intermediates. In route B, besides this, we use the Hbpp ligand where the pyrazolylic group has been protected with BOC in order to sterically influence the subsequent reactions.

Route A generates a ratio of *in* Ru−Cl **2a**/*out* Ru−Cl **2b** of 0.25 indicating that the *out* Ru−Cl isomer is clearly favored versus the *in* Ru−Cl isomer. In our case, with the Hbpp ligand, this is due to both steric and electronic effects. In *out* and *in* isomers, the degree of steric hindrance is due to the relative proximity of the trpy ligand to the hydrogen atoms H5 of the coordinated pyridyl moiety and H3b of the pyrazolylic N-bonded hydrogen atom respectively (see Figure 1 for atom labeling). The more constrained nature of the five-membered ring pyrazolylic group (C6N2N3 angle is 106.01°) over the six-membered ring pyridylic group (C1N1C5, 116.52°) is responsible for directing the H3b hydrogen atom farther away from the coordinating trpy ligand, thus leading to a situation with less steric hindrance in the case of the *out* isomer. Furthermore, the *out* Ru−Cl isomer is also favored due to the formation of a medium to weak hydrogen bond between the coordinated chloro ligand Cl1 and H5 (Cl1H5, 2.741 Å; Cl1H5C5, 123.48°; Cl1C5, 3.359 Å). This interaction is also consistent with the 2.84 ppm lower field shift observed in the ^{1}H NMR for H5 in the case of the *out* isomer with regard to the *in* (vide supra). For the *in* isomer, and again due to the more constrained five-membered pyrazolylic ring, the Cl would be situated farther away from H3b (simple trigonometric calculations yield a H3bCl1 distance of 3.248 Å; 50.7 pm larger than that for the *out* isomer) thus leading to a negligible hydrogen bonding contribution.

In route B, the pyrazolylic group of Hbpp is protected with the bulky BOC group. This allows us to reverse the contribution of steric effects in the *in* and *out* isomers while hydrogen bonding capabilities are practically not modified. The result is a modest but significant increase of the *in*/*out* ratio from 0.25 to 0.33 which reveals that the main factor influencing the *out* vs *in* preference is basically due to hydrogen bonding capacity of the Ru−Cl group. This is also in agreement with previous results published in the literature with the bis-pyridyl−pyrazine type of ligands[8b] where there is also a strong preference for the corresponding *out* Ru−Cl isomers.

Route B also has the advantage with regard to route A that the formation of dinuclear complexes is practically avoided and the formation of mononuclear complexes with two or more Hbpp ligands highly restricted. Thus, for route A the overall yield of *in* + *out* is 50.7% whereas for route B it rises to 80.6%.

Crystallographic data and selected bond distances and angles for complexes **2a**−**4a** and **4b** are reported in Table 1 and in the Supporting Information respectively; ORTEP views of their cationic moieties together with the labeling scheme are shown in Figure 1. In all cases, the Ru metal center has an octahedrally distorted type of coordination where the trpy ligand is bonded in a meridional manner, the Hbpp ligand acts in a chelate fashion, and finally the sixth coordination is occupied by the monodentate ligand. Bonding distances and angles are within the expected values for this type of complex.[10,11] Further details related to their crystal structures can be found in the Supporting Information.

(9) Sheldrick, G. M. *SHELXTL Crystallographic System Ver. 5.10*; Siemens Analytical X-ray Instruments, Inc.: Madison, WI, 1998.

(10) (a) Llobet, A. *Inorg. Chim. Acta* **1994**, *221*, 125. (b) Calligaris, M.; Carugo, O. *Coord. Chem. Rev.* **1996**, *153*, 83. (c) Laurent, F.; Plantalech, E.; Donnadieu, B.; Jiménez, A.; Hernández, F.; Martínez-Ripoll, M.; Biner, M.; Llobet, A. *Polyhedron* **1999**, *18*, 3321.

Table 2. pK_a and UV−Vis Spectroscopic Features in Aqueous Solutions[a] for the Complexes Described in the Present Paper

compd	assignment	λ_{max}, nm (ϵ, $M^{-1}\,cm^{-1}$)	pK_a
out-[RuCl(Hbpp)(trpy)]$^+$, **2a**	$\pi \rightarrow \pi^*$	274(41351), 321(40716)	
	$d\pi \rightarrow \pi^*$	367(12180), 394(10706), 493(8782)	
in-[RuCl(Hbpp)(trpy)]$^+$, **2b**	$\pi \rightarrow \pi^*$	274(36508), 316(42147)	
	$d\pi \rightarrow \pi^*$	378(9302), 485(8059)	
		out-**3a**	
			2.13, 6.88, 11.09 (Ru^{II})
			0.004, 2.78, 5.43 (Ru^{III})
$[Ru(H_2bpp)(trpy)(H_2O)]^{3+}$	$\pi \rightarrow \pi^*$	278(39358), 313(33841)	
	$d\pi \rightarrow \pi^*$	404(9622), 458(10682)	
$[Ru(Hbpp)(trpy)(H_2O)]^{2+}$	$d\pi \rightarrow \pi^*$	389(6252), 466(6279)	
$[Ru(bpp)(trpy)(H_2O)]^+$	$\pi \rightarrow \pi^*$	273(32318), 315(34384)	
	$d\pi \rightarrow \pi^*$	369(9649), 490(6686)	
[Ru(bpp)(OH)(trpy)]	$\pi \rightarrow \pi^*$	277(30307), 300(28296)	
	$d\pi \rightarrow \pi^*$	377(8779), 525(5028)	
		in-**3b**	
			1.96, 7.43, 12.20 (Ru^{II})
			0.04, 2.15, 6.58 (Ru^{III})
$[Ru(H_2bpp)(trpy)(H_2O)]^{3+}$	$\pi \rightarrow \pi^*$	313(25509)	
	$d\pi \rightarrow \pi^*$	394(8650), 458(9328)	
$[Ru(Hbpp)(trpy)(H_2O)]^{2+}$	$d\pi \rightarrow \pi^*$	386(6241), 460(6615)	
$[Ru(bpp)(trpy)(H_2O)]^+$	$\pi \rightarrow \pi^*$	314(27001)	
	$d\pi \rightarrow \pi^*$	378(7361), 382(7089), 474(5495)	
[Ru(bpp)(OH)(trpy)]	$\pi \rightarrow \pi^*$	309(22388)	
	$d\pi \rightarrow \pi^*$	364(8514), 405(6445), 517(5190)	
		out-**4a**	
			1.81, 6.77 (Ru^{II})
			0.11, 3.53 (Ru^{III})
$[Ru(H_2bpp)(trpy)(py)]^{3+}$	$\pi \rightarrow \pi^*$	279(43131), 313(37491)	
	$d\pi \rightarrow \pi^*$	392(11424), 439(9761)	
$[Ru(Hbpp)(trpy)(py)]^{2+}$	$\pi \rightarrow \pi^*$	272(38575), 279(38250)	
	$d\pi \rightarrow \pi^*$	383(9038), 454(6833)	
$[Ru(bpp)(trpy)(py)]^+$	$\pi \rightarrow \pi^*$	316(41215)	
	$d\pi \rightarrow \pi^*$	377(11316), 481(5893)	
in-[Ru(py)(Hbpp)(trpy)]$^{2+}$, **4b**	$\pi \rightarrow \pi^*$	273(30695), 314(40828)	
	$d\pi \rightarrow \pi^*$	372(9813), 472(6312), 503(5054)	

[a] For the **2a**, **2b**, and **4b** complexes, the spectra were registered in MeOH.

Spectroscopic Properties. The 1D and 2D NMR spectra of the Ru−Cl **2a**,**b**, and Ru−py **4a**,**b** complexes were registered in MeOH-d_4 or MeCN-d_3 and are presented and discussed in the Supporting Information. The UV−vis spectra of the *out* complexes **2a**−**4a** are presented in Figure 2. The corresponding *in* complexes **2b**−**4b** are relatively similar, and their main UV−vis spectroscopic features together with the rest of the complexes described in the present work are shown in Table 2 and as Supporting Information. Table 2 also reports acid−base properties of the complexes described here.

As can be seen in Figure 2, the complexes present ligand based $\pi-\pi^*$ bands below 340 nm and relatively intense bands above 340 nm assigned mainly to $d\pi-\pi^*$ transitions due to a series of MLCT transitions and their vibronic components.[12] For the Ru−Cl complexes the MLCT bands are shifted to longer wavelengths with regard to the Ru−OH_2 due to the relative destabilization of the $d\pi$(Ru) levels provoked by the chloro ligand. A similar band shifting is also observed for the Ru−OH complexes that are obtained under basic conditions (see inset Figure 2).

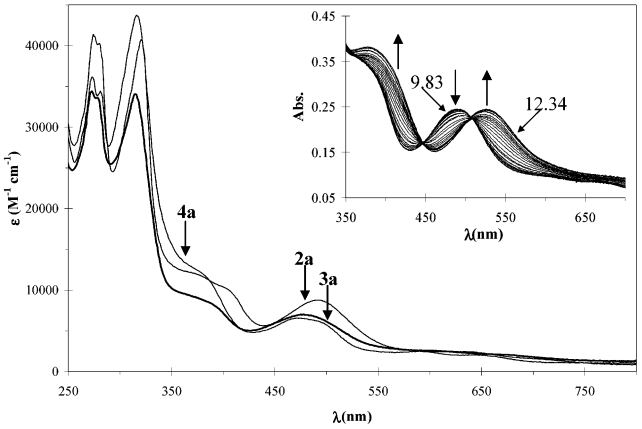

Figure 2. UV−vis spectra of **2a** and **4a** in MeOH and **3a** in a pH = 7.0 phosphate buffer. The inset shows the acid−base spectrophotometric titration of **3a** upon consecutive additions of 5 μL of NaOH 4.0 M. (Initial pH = 9.60; subsequent additions: pH = 9.83, 9.94, 10.08, 10.15, 10.26, 10.36, 10.45, 10.60, 10.72, 10.84, 11.05, 11.20, 11.35, 11.49, 11.61, 11.71, 11.79, 11.91, 12.02, 12.10, 12.19, 12.26, 12.34.)

The Ru−aqua complex, **3a**, has three sites that can be protonated or deprotonated within the pH range 0−13 which are the noncoordinated pyridylic group (pyr) and the pyrazolylic group (pzH) of the Hbpp ligand and the aqua group that acts as a ligand and that is directly bonded to the Ru metal center. A spectrophotometric acid−base titration of **3a** (see Supporting Information) was carried out

(11) (a) Anda, C.; Llobet, A.; Motekaitis, R.; Riebenspies, J.; Martell, A. E. *Inorg. Chem.* **2000**, *39*, 2986. (b) Lehn, J. M.; Meric, R.; Vigneron, J. P.; Bkouche-Waksman, I.; Pascard, C. *Chem. Commun.* **1991**, 62.
(12) (a) Barkawi, K.; Llobet, A.; Meyer, T. J. *J. Am. Chem. Soc.* **1988**, *110*, 7751. (b) Rodriguez, M.; Romero, I.; Llobet, A.; Deronzier, A.; Biner, M.; Parella, T.; Stoeckli-Evans, H. *Inorg. Chem.* **2001**, *40*, 4150.

in order to calculate their pK_a which led to the following values:

$$[Ru^{II}(H_2bpp)(trpy)(H_2O)]^{3+} \xrightarrow[pK_{a1}(Ru^{II}) = 2.13]{} [Ru^{II}(Hbpp)(trpy)(H_2O)]^{2+} + H^+ \quad (1)$$

$$[Ru^{II}(Hbpp)(trpy)(H_2O)]^{2+} \xrightarrow[pK_{a2}(Ru^{II}) = 6.88]{} [Ru^{II}(bpp)(trpy)(H_2O)]^{+} + H^+ \quad (2)$$

$$[Ru^{II}(bpp)(trpy)(H_2O)]^{+} \xrightarrow[pK_{a3}(Ru^{II}) = 11.09]{} [Ru^{II}(bpp)(OH)(trpy)] + H^+ \quad (3)$$

The assignment of the protons to the different protonatable groups of the **3a** complex has been made by comparison with related complexes that had only one type of protonation site.[13]

Another set of acid−base spectrophotometric titrations can also be performed with the *in* Ru−OH_2 **3b** isomer that gives the following values: p$K_{a1}(Ru^{II}) = 1.96$, p$K_{a2}(Ru^{II}) = 7.43$, and p$K_{a3}(Ru^{II}) = 12.20$. These values are relatively similar to the *out* **3a** case except for pK_{a3} that is 1.1 log units higher indicating that it is less acidic. This can be attributed to the possibility of hydrogen bonding between the Ru−aqua and the pyrazolate group of the Hbpp ligand that cannot take place in the *out* isomer. The Ru−py complexes **4a** and **4b** also have acid−base properties, and their pK_a values have also been calculated through spectrophotometric titrations in a similar manner (see Table 2).

Redox Properties. The redox properties of the complexes described in the present work were investigated by means of cyclic voltammetric and coulombimetric techniques. All complexes display a pH dependency of their redox properties due to their multiple protonation sites as has been described in the previous section.

For the *out* Ru−aqua complex **3a** at pH = 1.0, only one chemically reversible and electrochemically quasireversible wave is observed at $E_{1/2} = 0.614$ V versus SSCE, ($E_{p,a} = 0.659$ V; $E_{p,c} = 0.570$ V; $\Delta E = 89$ mV) which is due to the Ru(III)/Ru(II) couple.

$$[Ru^{III}(Hbpp)(trpy)(H_2O)]^{3+} + 1e^- + 1H^+ \rightarrow [Ru^{II}(H_2bpp)(trpy)(H_2O)]^{3+} \quad (4)$$

At basic pH, two redox processes can be detected as can be seen in Figure 3. For instance, at pH = 11.5 two chemically reversible redox waves at $E_{1/2} = -0.001$ V and $E_{1/2} = 0.374$ V are observed. The first wave is assigned to the Ru(III)/Ru(II) couple ($E_{p,a} = -0.036$ V; $E_{p,c} = 0.034$ V; $\Delta E = 70$ mV) and the second to the Ru(IV/III) couple ($E_{p,a} = 0.414$ V; $E_{p,c} = 0.334$ V; $\Delta E = 80$ mV).

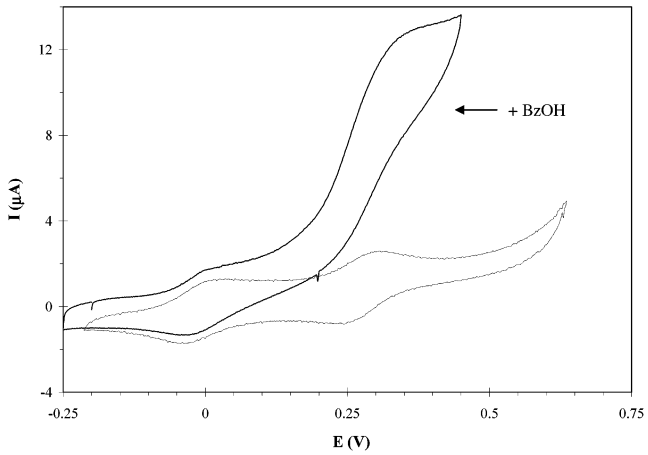

Figure 3. Cyclic voltammetries for **3a** (0.15 mM) at 0.02 V s^{-1} in aqueous solution (pH = 12.0). The electrocatalytic effect of adding 0.2 M benzyl alcohol is also shown.

$$[Ru^{IV}(bpp)(O)(trpy)]^{+} + 1e^- + 1H^+ \rightarrow [Ru^{III}(bpp)(OH)(trpy)]^{+} \quad (5)$$

The complete redox behavior of **3a** as a function of pH is shown in the Pourbaix diagram depicted in Figure 4A. The figure shows the experimental $E_{1/2}$−pH values obtained from CV.

The relation between the Ru(III)/Ru(II) redox potentials and the three acid dissociation constants of complex **3a** species is given by the equation[5c]

$$E_{1/2}(III/II) = E_{1/2}^{\circ}(III/II) + 0.059 \times \log \frac{[H^+]^3 + K_{a1}(Ru^{II})[H^+]^2 + K_{a1}(Ru^{II})K_{a2}(Ru^{II})[H^+] + K_{a1}(Ru^{II})K_{a2}(Ru^{II})K_{a3}(Ru^{II})}{[H^+]^3 + K_{a1}(Ru^{III})[H^+]^2 + K_{a1}(Ru^{III})K_{a2}(Ru^{III})[H^+] + K_{a1}(Ru^{III})K_{a2}(Ru^{III})K_{a3}(Ru^{III})} \quad (6)$$

where $E_{1/2}^{\circ}$(III/II) is the standard redox potential of the couple Ru(III)/Ru(II). Nonlinear least-squares analysis[14] of the experimental data has provided the best fit curves shown in Figure 4A. In this fit, the pK_a values for the Ru(II) oxidation state, calculated via acid−base spectrophotometric titration, were taken as fixed values. Further, $K_{a1}(Ru^{III})$ was not allowed to have values higher than 1.0, since for higher values it did not give any substantial change into the fit. Thus, in this way we were able to calculate the dissociation constants of the different species with the Ru metal center in the oxidation state III: p$K_{a1}(Ru^{III}) = 0.01$, p$K_{a2}(Ru^{III}) = 2.78$, p$K_{a3}(Ru^{III}) = 5.43$ ($R = 2.517 \times 10^{-4}$).

For the Ru−OH_2 polypyridylic type of complexes, the pK_a value for the proton of the aqua ligand bonded to the Ru metal center decreases by 8−10 log units upon changing from oxidation state II to III[6,13] whereas for polypyridylic

(13) (a) Haga, M.; Ano, T.; Ishizaki, T.; Kano, K.; Nozaki, K.; Ohno, T. *J. Chem. Soc., Dalton Trans.* **1994**, 263−272. (b) Haga, M.; Ali, M. M.; Koseki, S.; Fujimoto, K.; Yoshimura, A.; Nozaki, K.; Ohno, T.; Nakajima, K.; Stufkens, D. J. *Inorg. Chem.* **1996**, *35*, 3335. (c) Dovletoglou, A.; Ajao Adeyemi, S.; Meyer, T. J. *Inorg. Chem.* **1996**, *35*, 4120. (d) Ayers, T.; Caylor, N.; Ayers, G.; Godwin, C.; Hathcock, D. J.; Stuman, V.; Slattery, S. J. *Inorg. Chim. Acta* **2002**, *328*, 33.

(14) The fit was obtained through least-squares analysis. The best fit was obtained by minimizing the function $R = \sum(E_{1/2}^{calcd} - E_{1/2}^{obs})^2 / \sum(E_{1/2}^{obs})^2$.

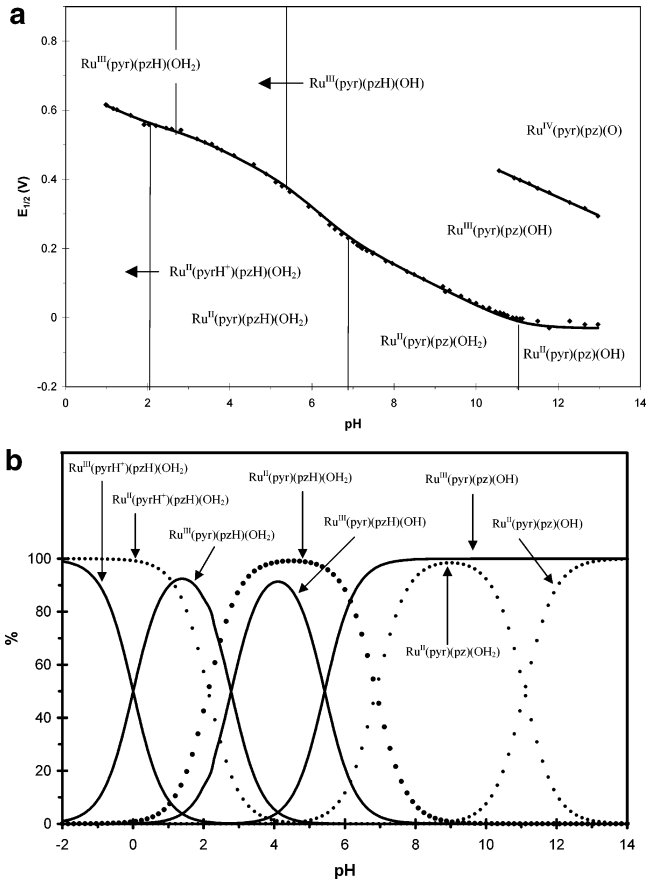

Figure 4. (A) $E_{1/2}$ vs pH or Pourbaix diagram of **3a**. The pH−potential regions of stability for the various oxidation states and their dominant proton compositions are indicated. We are using abbreviations which display the proton contents of the different sites of the complex, which can change within the 0−14 pH range. In its neutral form, these are the free noncoordinated pyridyl group of the Hbpp ligand (pyr), the pyrazolate group also of the Hbpp ligand (pzH), and the aqua ligand directly bonded to the Ru metal center (H_2O). Therefore, for example for *out*-$[Ru^{II}(H_2bpp)(trpy)(H_2O)]^{3+}$ we use the abbreviation "$Ru^{II}(pyrH^+)(pzH)(OH_2)$" which indicates that the metal is in its oxidation state II, the free pyridyl group is protonated, the pyrazolylic group is also protonated, and the bonded aqua ligand acts as neutral ligand. The pK_a values are shown by the vertical solid lines in the various E−pH regions, and their numerical values are displayed in Table 2. (B) Species distribution diagram as a function of pH, for the species derived from **3a** under its different protonated forms. Dotted lines refer to Ru in oxidation state II while the solid lines refer to Ru in oxidation state III.

Ru complexes with no aqua ligands the same shift is about two log units.[5c] Therefore, in our particular case the first p$K_{a1}(Ru^{III})$ is assigned to the protonation of the pyridylic group, the p$K_{a2}(Ru^{III})$ to the Ru−aqua ligand and the p$K_{a3}(Ru^{III})$ to the pyrazolylic group of the Hbpp ligand.

With the pK_a values precisely known, a species distribution diagram as function of pH and oxidation state can be drawn and is presented in Figure 4B. The diagram gives a concise idea of the regions of stability of the differently protonated species as well as their coexistence and shows how upon increasing the oxidation state, the zones of stability of the differently protonated species shift to lower pH.

It is also interesting to compare the redox potentials of our Ru−aqua complexes with those previously reported in the literature.[10a,12b] For instance, the $[Ru(trpy)(bpy)(H_2O)]^{2+}$ complex (bpy is 2,2′-bipyridine) at pH = 7 possesses an $E_{1/2}$(IV/III) = 0.62 V and an $E_{1/2}$(III/II) = 0.49 V with a $\Delta E_{1/2}$(IV/III−III/II) = 130 mV. The substitution of bpy by a strong σ-donor ligand such as acetylacetonate (acac) to yield the corresponding $[Ru(acac)(trpy)(H_2O)]^+$ complex produces a stabilization of the Ru(IV) and Ru(III) oxidation states with regard to the bpy complex already mentioned. This stabilization is now responsible for the strong decrease of the III/II couple while the IV/III is much less affected (pH = 7: $E_{1/2}$(IV/III) = 0.56 V, $E_{1/2}$(III/II) = 0.19 V, $\Delta E_{1/2}$(IV/III−III/II) = 370 mV) indicating that the oxidation states IV and III are affected in a relatively similar manner by the $acac^-$ ligand. A similar phenomenon is also observed for complex **3a** (pH = 7: $E_{1/2}$(IV/III) = 0.61 V, $E_{1/2}$(III/II) = 0.24 V, $\Delta E_{1/2}$(IV/III−III/II) = 370 mV) showing that the anionic nature of the bpp^- ligand also produces a strong stabilization of oxidation states IV and III.

The redox behavior of complex **3b** parallels that of **3a** with slight variations. The Pourbaix diagram is presented in the supplementary information and the calculated pK_a values for oxidation states II and III are displayed in Table 2.

Coulombimetric analyses at different pH and at an applied potential E_{app} close to the corresponding $E_{1/2}$(III/II) values were performed for complexes **3a** and **3b** with approximately 1 mol of electrons per mol of complex. However, the CVs of the final solutions present electrochemical features different from the initial ones even though in some cases the UV−vis spectroelectrochemical analysis gave isobestic points. This clearly indicates that Ru(III) species derived from **3a** or **3b** are stable in the CV time scale but not in the coulombimetric time scale. The nature of the oxidized species is currently being investigated. This instability of the oxidized species highlights the importance of the Pourbaix diagram and its simulation that allows us to calculate the corresponding pK_a values for Ru(III) species since they could not be obtained through conventional acid−base spectrophotometric titrations.

Figure 3 shows the effect of performing a CV of **3a** at a scan rate of 20 mV/s at pH = 12.0 in the absence and presence of 0.20 M benzyl alcohol (BzOH). When the alcohol is present, there is a strong enhancement of the anodic peak of the second wave denoting the presence of an electrocatalytic process. Thus, when the Ru^{IV}═O active species is generated in the second wave it then rapidly oxidizes the alcohol, presumably to benzaldehyde.[15] A second-order rate constant, k_{cat} = 17.1 M^{-1} s^{-1} is obtained from the mathematical simulation (see Supporting Information) of the process using DigiSim.[16] This value is of the same order of magnitude as those for other polypyridylic Ru^{IV}═O complexes described previously in the literature,[8b,17] capable of oxidizing the same substrate under similar conditions, with k_{cat} values ranging from 6.0 to 30.8 M^{-1}•s^{-1}.

As has been shown, the availability of two protonation sites beside the catalytically active Ru═O group that can be

(15) (a) Polcyn, D. S.; Shain, I. *Anal. Chem.* **1966**, *38*, 376. (b) Bard, A. J.; Faulkner, L. R. In *Electrochemical Methods*; Wiley: New York, 1980.
(16) *DigiSim for Windows 95*, version 3.05; Bioanalytical Systems.
(17) (a) Lebeau, E. L.; Meyer, T. J. *Inorg. Chem.* **1999**, *38*, 2174. (b) Gerli, A.; Reedijk, J.; Lakin, M. T.; Spek, A. L. *Inorg. Chem.* **1995**, *34*, 1836.

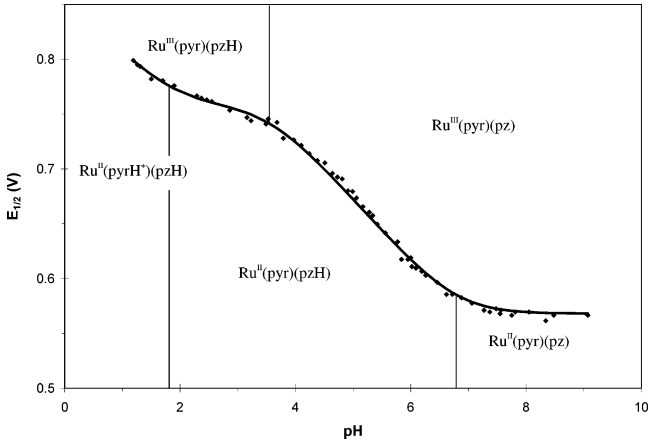

Figure 5. $E_{1/2}$ vs pH or Pourbaix diagram of **4a**. (See Figure 4 caption for details.)

generated from **3a** and **3b** makes these complexes attractive for studying proton coupled electron transfer processes and for designing novel oxidation catalysts where the thermodynamic properties of the Ru=O group can be tuned through pH.

The redox properties of the Ru−py **4a** and **4b** also parallel those of the aqua complexes except that in this case there are only two protonation sites and only one redox process corresponding to the Ru(III)/Ru(II) couple. The pH dependency of the redox potentials of the *out* Ru−py **4a** isomer is presented in Figure 5. The same methodology as that previously applied was used for the simulation of the Pourbaix diagram taking into account that now there are only two acidic protons. Thus the following equation was used:

$$E_{1/2}(\mathrm{III/II}) = E_{1/2}^{\circ}(\mathrm{III/II}) + 0.059 \times \log \frac{[\mathrm{H}^+]^2 + K_{a1}(\mathrm{Ru^{II}})[\mathrm{H}^+] + K_{a1}(\mathrm{Ru^{II}})K_{a2}(\mathrm{Ru^{II}})}{[\mathrm{H}^+]^2 + K_{a1}(\mathrm{Ru^{III}})[\mathrm{H}^+] + K_{a1}(\mathrm{Ru^{III}})K_{a2}(\mathrm{Ru^{III}})} \quad (7)$$

The results obtained are presented in Table 2. It is worth noting here that the Ru(III)/Ru(II) potential for **4a** can be changed by more than 200 mV by simply changing the pH of the solution, and thus, it could potentially be used as a pH-induced redox switch.[5,18]

Acknowledgment. This research has been financed by MCYT of Spain through Project BQU2000-0458. A.L. is grateful to CIRIT Generalitat de Catalunya (Spain) for the Distinction award and the aid SGR2001-UG-291. A.L. also thanks Johnson and Matthey for a $RuCl_3 \cdot xH_2O$ loan. C. S. is grateful for the award of a doctoral grant from CIRIT.

Supporting Information Available: CIF files together with additional spectroscopic and electrochemical data. This material is available free of charge via the Internet at http://pubs.acs.org. The supplementary crystallographic data for this paper (CCDC 213376, CCDC 213377, CCDC 213378 and CCDC 213379) can also be obtained free of charge via www.ccdc.cam.ac.uk/conts/retrieving.html (or from the Cambridge Crystallographic Data Centre, 12, Union Road, Cambridge CB2 1EZ, U.K. Fax: +44 1223 336033. E-mail: deposit@ccdc.cam.ac.uk). This material is available free of charge via the Internet at http://pubs.acs.org.

IC0346836

(18) Lomoth, R.; Haupl, T.; Johanson, O.; Hammarstrom, L. *Chem. Eur. J.* **2002**, *8*, 102.